



Northeast African temperature variability since the Late Pleistocene



Shannon E. Loomis^{a,*}, James M. Russell^a, Henry F. Lamb^b

^a Brown University, Department of Earth, Environmental and Planetary Sciences, 324 Brook St., Box 1846, Providence, RI 02912, USA

^b Aberystwyth University, Department of Geography and Earth Sciences, Aberystwyth SY23 3DB, UK

ARTICLE INFO

Article history:

Received 12 August 2014

Received in revised form 15 January 2015

Accepted 1 February 2015

Available online 8 February 2015

Keywords:

Tropical paleoclimate

East Africa

GDGT

Paleotemperature

Holocene

Lake Tana

ABSTRACT

The development and application of lacustrine paleotemperature proxies based on microbial membrane lipid structures, including the TEX₈₆ and branched glycerol dialkyl glycerol tetraether (brGDGT) paleothermometers, have greatly advanced our understanding of the late-glacial and postglacial temperature history of Africa. However, the currently available records are from equatorial and southern hemisphere sites, limiting our understanding of the spatial patterns of temperature change. Here we use the brGDGT paleotemperature proxy to reconstruct Late Pleistocene and Holocene temperatures from Lake Tana, Ethiopia (12°N, 37°E). Following the termination of Heinrich Stadial 1 at ~15 ka, Lake Tana experienced a 3.7 °C oscillation over 1.2 ky. Temperatures then increased abruptly by nearly 7 °C between 13.8 and 13.0 ka, followed by a slow warming trend that peaked during the mid Holocene. Temperatures subsequently cooled from ~6 ka to ~0.4 ka. These data indicate that temperature at Lake Tana was sensitive to climate changes caused by variations in the Atlantic Meridional Overturning Circulation during the Late Pleistocene, as well as to regional hydroclimatic changes and reorganizations of the monsoons. Our record suggests that late-glacial temperature changes in northeast Africa were linked to high-latitude northern hemispheric climate processes, but that subsequent post-glacial temperature variations were strongly influenced by tropical hydrology.

© 2015 Elsevier B.V. All rights reserved.

1. Introduction

Quantitative paleoclimate reconstructions are crucial for testing global climate models and for understanding the drivers of past and future climate change (Schmittner et al., 2011; Shakun et al., 2012). Despite the importance of tropical temperatures in driving atmospheric convection, continental temperature reconstructions from the tropics are very limited. This is largely due to difficulties in reconstructing tropical continental temperatures using conventional proxies, such as tree rings (e.g., Gebrekirstos et al., 2009), pollen (e.g., Coetzee, 1967), and stable isotopes (e.g., Thompson et al., 2002). In recent years, the development of glycerol dialkyl glycerol tetraether (GDGT) paleothermometry has greatly enhanced our ability to reconstruct terrestrial tropical temperatures and the thermal history of Africa in particular. The TEX₈₆ proxy (TetraEther indeX of tetraethers with 86 carbon atoms; Schouten et al., 2002), based on the relative abundances of isoprenoidal GDGTs produced by mesophilic archaea, has been used to reconstruct past temperature in Lakes Malawi (Powers et al., 2005; Woltering et al., 2011), Tanganyika (Tierney et al., 2008), Turkana (Berke et al., 2012b), Victoria (Berke et al., 2012a), and Albert (Berke et al., 2014). However, TEX₈₆ is only applicable in some large lakes (Powers et al., 2010), limiting its ability as a widespread terrestrial paleotemperature proxy.

Branched GDGTs (brGDGTs) are produced by heterotrophic acidobacteria (Weijers et al., 2006, 2010; Sinninghe Damsté et al., 2011, 2014) and their relative abundances are also temperature dependent (Weijers et al., 2007a). BrGDGTs are much more abundant than isoprenoidal GDGTs in sediments from smaller lakes (e.g., Tierney and Russell, 2009; Powers et al., 2010; Loomis et al., 2014a), and they have been used to reconstruct paleotemperatures using lake sediments at temperate (Fawcett et al., 2011; Niemann et al., 2012), subtropical (Woltering et al., 2014), and tropical (Loomis et al., 2012) latitudes. GDGT-based temperature records from equatorial East Africa have begun to illuminate the region's thermal history and generally exhibit coherent trends and amplitudes of change on orbital timescales. For instance, these records suggest that, compared to pre-industrial period, temperatures were 3–5 °C cooler at the last glacial maximum (LGM; Powers et al., 2005; Tierney et al., 2008; Loomis et al., 2012) and between 1 and 3 °C warmer during the mid-Holocene, ca. 7–5 ka (Powers et al., 2005; Tierney et al., 2008; Berke et al., 2012b; Loomis et al., 2012), similar to findings from TEX₈₆ reconstructions from the region's large lakes.

Thus far, all of the published paleotemperature records from eastern Africa are from equatorial regions or the southern hemisphere, hindering our understanding of inter-hemispheric temperature variability on longer timescales. In order to better understand the climatic controls on northeastern African temperature variability and cross-equatorial spatial gradients from the late Pleistocene through the Holocene, we have reconstructed paleotemperatures from Lake Tana, Ethiopia, using the brGDGT paleotemperature proxy.

* Corresponding author at: University of Texas at Austin, Department of Geological Sciences, 1 University Station C1160, Austin, TX 78712, USA. Tel.: +1 512 232 5762.

E-mail address: sloomis@jsg.utexas.edu (S.E. Loomis).

2. Materials and methods

2.1. Site information

Lake Tana (12.0°N, 37.3°E; 1830 m elevation; Fig. 1) is a large (3156 km²) but shallow (maximum depth = 14 m, mean depth = 9 m) freshwater lake located on the basaltic plateau of northeastern Ethiopia. It is a slightly alkaline (pH = 8), oligo-mesotrophic lake (Wood and Talling, 1988) with four major inflows that contribute >95% of the riverine input, and one outflow, the Blue Nile (Lamb et al., 2007).

Mean annual air temperature at Lake Tana is 18.8 °C, and total annual precipitation is 1450 mm (Kebede et al., 2006). Atmospheric temperature seasonality at Lake Tana is relatively weak, with monthly temperatures ranging from 16.3 °C in December to 21.3 °C in May (Kebede et al., 2006). Precipitation seasonality, however, is extreme at Lake Tana due to its position near the northern limit of the annual migration of the Inter-tropical Convergence Zone (ITCZ), with monthly average rainfall ranging from 2 mm in February to 430 mm in July (Kebede et al., 2006). Wind direction also varies seasonally, with southerly flow during boreal summer and northeasterly flow during boreal winter due to the east African and Indian monsoons (Wondie et al., 2007).

Mean surface water temperature at Lake Tana is 22.9 ± 0.7 °C, and water temperature does not correlate with increased runoff or primary productivity (Wondie et al., 2007). The large surface area of the lake relative to its depth, combined with diurnal atmospheric temperature variations and wind strength, inhibits the development of a thermocline in the lake, resulting in minimal seasonal stratification (Wood and Talling, 1988; Wondie et al., 2007). Given the local climate and surface water temperature measurements, hydrodynamic modeling predicts that bottom water temperatures at the deepest point (14 m) are ~1 °C colder than surface water temperatures (Dargahi and Setegn, 2011).

2.2. Core collection, sedimentology, and chronology

In October 2003, a 10.3 m sediment core (03TL3) was recovered from 13.8 m water depth near the center of the lake using a Livingstone piston corer. This core has four distinct lithological units (Lamb et al., 2007). Unit 1 (1030–1000 cm) is a dark gray silt with an organic matter content of 9–22%, and is overlain by Unit 2 (1000–955 cm), a dark brown herbaceous peat with an organic matter content of 30–70%. Unit 3 (955–937) has sharp upper and lower contacts, is comprised of slightly calcareous silt and organics, and diatom evidence suggests that it was likely deposited in waters with higher conductivity (3500 µS/cm) (Lamb et al., 2007).

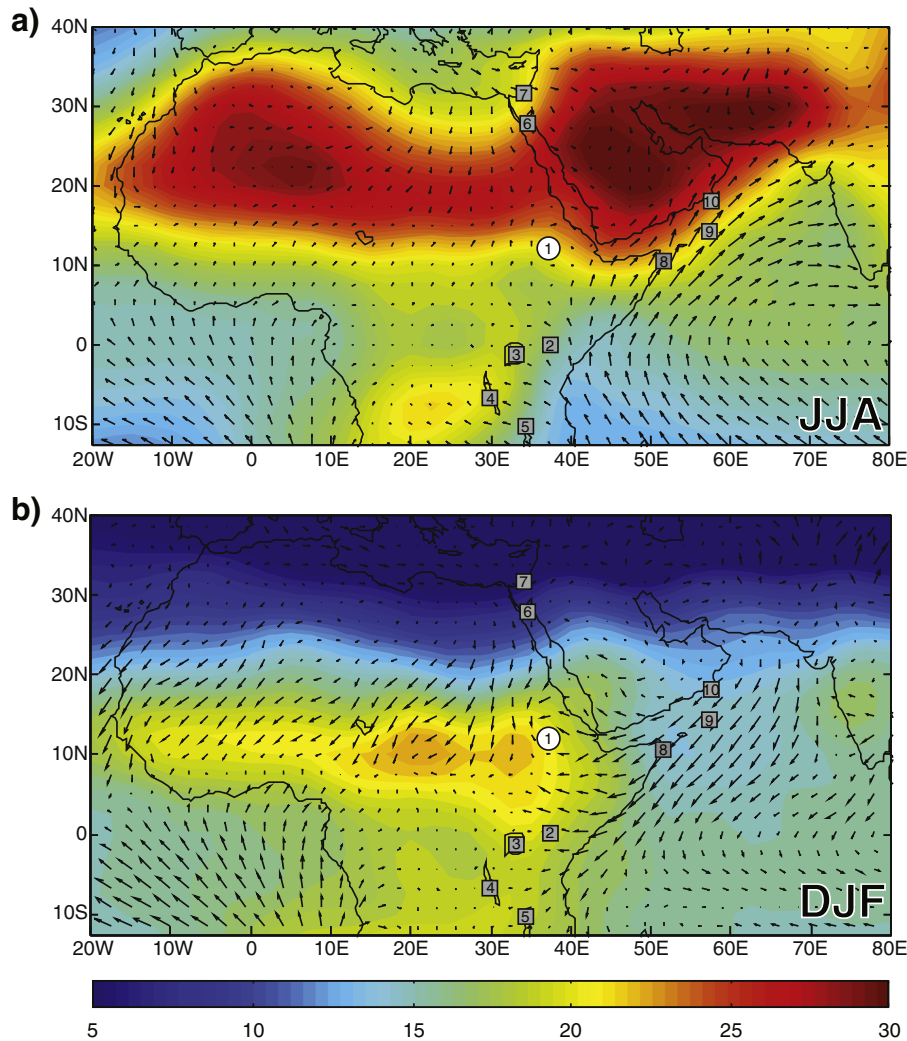


Fig. 1. Map of average surface winds and air temperatures at 850 mb. a) June, July, and August (JJA), b) December, January, and February (DJF). White dot (1) marks the location of Lake Tana core 03TL3 (this study, Marshall et al., 2011, and Costa et al., 2014), and gray boxes mark the locations of other paleoclimate records mentioned in the text: 2: Sacred Lake, (Loomis et al., 2012); 3: Lake Victoria (Berke et al., 2012a); 4: Lake Tanganyika (Tierney et al., 2008); 5: Lake Malawi (Powers et al., 2005); 6: Red Sea, GeOB 5844-2 (Arz et al., 2003); 7: Eastern Mediterranean, GeOB 7702-3 (Castañeda et al., 2010); 8: Arabian Sea, 905P (Zonneveld et al., 1997); 9: Arabian Sea, 74KL (Huguet et al., 2006); 10: Arabian Sea, ODP 723A (Naidu and Malmgren, 1996, 2005).

Unit 4 (937–0 cm) is a uniform fine gray diatomaceous silt, containing lower organic matter and higher magnetic susceptibility than Units 1–3. Core chronology is derived from mixed effect regression (Heegaard et al., 2005) on 19 radiocarbon ages (Marshall et al., 2011). Errors (1σ) on the age model range from 120 years over the top 200 cm of the core to 500 years at the base of Unit 4.

2.3. Sample preparation and GDGT analysis

2 cm-thick subsamples were collected from core 03TL3 every 15 cm (~235 yr) and were transported to Brown University for preparation and analysis. Sample preparation followed that of Loomis et al. (2012). Briefly, samples were freeze-dried then homogenized with a mortar and pestle. Lipids were extracted using a Dionex 350 Accelerated Solvent Extractor (ASE) using 9:1 dichloromethane (DCM):methanol (MeOH). Extracts were separated into non-polar and polar fractions with an Al_2O_3 column using 9:1 hexane:DCM and 1:1 DCM:MeOH, respectively, as eluents. The polar fractions were filtered through a 0.22 μm glass fiber filter and analyzed using high performance liquid chromatography/atmospheric pressure chemical ionization-mass spectrometry (HPLC/APCI-MS).

To explore potential changes in microbial ecology through time, we quantified the relative abundance of branched to isoprenoidal tetraethers (BIT; Hopmans et al., 2004) using the following equation:

$$BIT = (Ia + Ila + IIIa)/(Ia + Ila + IIIa + cren) \quad (1)$$

where the Roman numerals refer to structures in Fig. 2. Mean annual air temperature (MAAT) was reconstructed using the East African stepwise forward selection (SFS) calibration:

$$MAAT = 22.7 - 33.58 * IIIa - 12.88 * Ila - 418.53 * Iic + 86.43 * Ib \quad (2)$$

of Loomis et al. (2012).

Analytical error was quantified by running 10% of samples in duplicate, and reconstructed MAAT error was determined through bootstrapping the reconstruction with the East African lakes calibration data (Loomis et al., 2012). Duplicate samples show an average analytical BIT error of 0.0009, while the average analytical reconstructed MAAT error is 0.08 °C. Bootstrapped MAAT error on individual samples ranges from 0.2 to 1.3 °C, with an average of 0.9 °C (Fig. 3a).

3. Results and discussion

3.1. Production and distribution of GDGTs in Lake Tana

Both branched and isoprenoidal GDGTs were detected in all samples from Lake Tana core 03TL3. BIT values range from 0.29 to 1.00 (mean = 0.71, standard deviation = 0.15; Fig. 3b), with the highest values located in the silts and peats that comprise Units 1–3 at the base of the core (BIT = 0.96–1.00). BIT values remain relatively constant from the base of Unit 4 to ~300 cm depth (mean = 0.75, standard deviation = 0.11), but become more variable (standard deviation = 0.17) and have a lower mean (0.55) than the rest of the unit above 300 cm.

BrGDGT reconstructed temperatures range from 11.2 to 21.9 °C (Fig. 3a). Reconstructed temperatures are lowest below 800 cm, shift to higher temperatures between 800 and 775 cm, and peak near 500 cm. This trend is interrupted by large negative reconstructed temperature excursions in samples with BIT < 0.5 (133–59 cm). The relationship between BIT and reconstructed temperatures could suggest that the environmental conditions and/or ecological changes associated with increased isoprenoidal GDGTs relative to brGDGTs affects the relative abundances of brGDGTs and thereby reconstructed temperatures. Before making paleoclimatic interpretations of the Lake Tana brGDGT temperature record, it is important to understand the environmental controls on the production of brGDGTs and their depositional history.

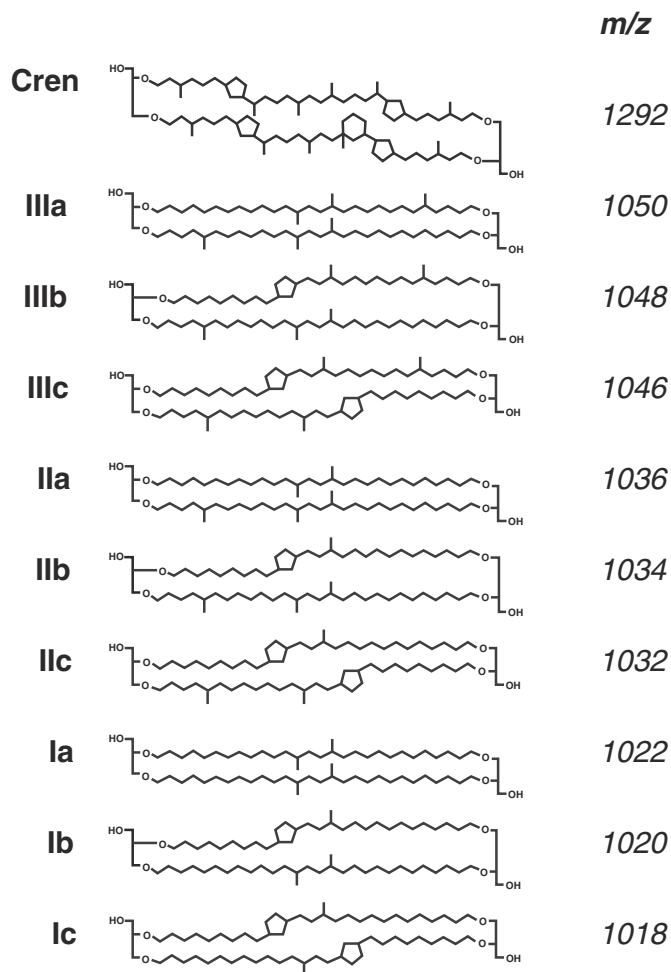


Fig. 2. Structures of GDGTs discussed in the text, including the isoprenoidal crenarchaeol (cren) and the brGDGTs (IIIa–Ic).

3.1.1. Influence of paleolimnology and sediment lithology on brGDGT distributions

BrGDGTs have been detected in peat (e.g., Sinninghe Damsté et al., 2000), soil (e.g., Weijers et al., 2007a), lake sediments (e.g., Tierney et al., 2010), and marine sediments (e.g., Weijers et al., 2007b). Although some studies have concluded that brGDGTs in particular lakes are derived from soil runoff (Niemann et al., 2012; Woltering et al., 2014), the majority of studies (Sinninghe Damsté et al., 2009; Tierney and Russell, 2009; Loomis et al., 2011, 2014b; Tierney et al., 2012; Wang et al., 2012; Buckles et al., 2014a,b) – including all of those that have been performed in the tropics – have found that the concentrations and distributions of brGDGTs in lake sediments are substantially different from surrounding soils, indicating that in most lacustrine environments, brGDGTs are predominantly derived from in situ production. The differences in brGDGT distributions in lake sediments and surrounding soils can result in differences between reconstructed temperatures in soils and adjacent lake sediments; for instance, offsets of up to 10 °C are commonly observed between soils and lake sediment in East Africa (Tierney et al., 2010; Loomis et al., 2011). Thus, changes in catchment hydrology, soil erosion, and lake sedimentation – such as large variations in the inputs of soil-derived organic matter – have the potential to affect reconstructed temperatures from brGDGTs. While the reason for these differences between brGDGTs in lakes and soils is still unknown, it is possible that it is related to changes in water or gas saturation in the environment (Loomis et al., 2011) and/or differences in the microbial ecology between lake and soil environments (Loomis et al., 2014a).

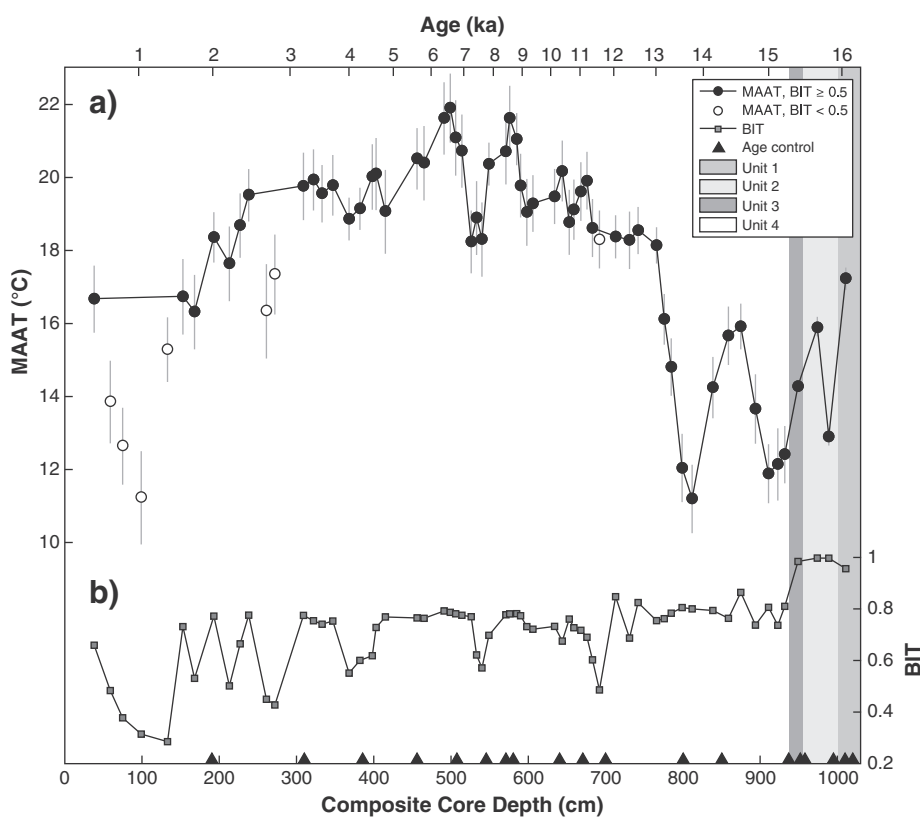


Fig. 3. GDGT records from Lake Tana core 03TL3. a) Reconstructed mean annual air temperature (MAAT). Black circles are samples with BIT values ≥ 0.5 , open circles are samples with BIT values < 0.5 . Bootstrapped 1σ errors on reconstructed temperatures are indicated by the gray lines. b) BIT record. Black triangles along the x-axis mark the depths of age control points (Marshall et al., 2011). Background is shaded to represent the different lithological units (Lamb et al., 2007) described in the text: medium gray for Unit 1 (dark gray silt; organic matter = 9–22%), light gray for Unit 2 (dark brown herbaceous peat; organic matter = 30–70%), dark gray for Unit 3 (calcareous silt; deposition conductivity = 3500 $\mu\text{S}/\text{cm}$), and white for Unit 4 (uniform fine gray diatomaceous silt; low organic matter and high magnetic susceptibility).

The basal units of core 03TL3 include organic-rich silts, peats, and calcareous muds that could signal varying sources of brGDGTs to these sediments, including not only soil vs. lacustrine production, but also in situ production of brGDGTs in peat. A greenhouse experiment carried out on peat bogs demonstrated that brGDGT distributions in surface peat layers change in response to variations in mean air temperature (Huguet et al., 2013). However, there is also good evidence of in situ production of brGDGTs within deeper peat layers (Weijers et al., 2009; Peterse et al., 2011), which may potentially alter the brGDGT distributions that were present when these sections were exposed and responding to surface air temperatures, thereby biasing the temperature signal. Unfortunately, widespread calibration studies have yet to be carried out on peat, inhibiting our understanding of the temperature/brGDGT relationship in peat samples.

To examine the potential for varying brGDGT sources to affect reconstructed temperatures in the Lake Tana core, we compared the fractional abundances of brGDGTs from Units 1–3 to Unit 4 using one way analysis of variance (ANOVA) testing. We find that the fractional abundances of brGDGTs with zero (IIIa, IIa, and Ia) and one cyclopentyl rings (IIIb, IIb, Ib) are significantly different ($p \leq 0.002$) between these stratigraphic units. As several of these compounds are important to our temperature calibration, and in light of the possibility of changing microbial sources of brGDGTs in the variable depositional environments represented by these units, we limit our temperature interpretation of reconstructed temperatures in this core to Unit 4 (937–0 cm).

While the lithology and percent organic matter ($9.5 \pm 1.1\%$) remain fairly constant throughout Unit 4 (Marshall et al., 2011), the Ti record shows substantial variability, including an abrupt increase in Ti concentrations at 700 cm (~12 ka), a negative Ti oscillation between 515 and 575 cm (~7–8.5 ka), and a decrease in Ti concentrations at 400 cm (~4.5 ka) (Fig. 4c). These large changes in Ti concentration indicate

variations in soil runoff (Marshall et al., 2011), which has the potential to change the relative proportions of allochthonous vs. autochthonous brGDGTs in the lake sediments. However, the large and abrupt shifts in Ti concentrations at 700 cm (12 ka) and 400 cm (4.5 ka) do not correspond to large changes in reconstructed temperature (Fig. 4a), indicating that the effects of changing delivery of soil-derived brGDGTs from the catchment on our temperature reconstruction are limited. The negative Ti oscillation between 515 and 575 (7–8.5 ka), however, is contemporaneous with a negative temperature oscillation (Fig. 4), and thus, we cannot rule out a changing brGDGT source during this interval. In spite of this, we believe that these oscillations are a result of climate variability (see Section 3.2.2) rather than a change in runoff, as other large Ti changes are not correlated with temperature variability.

Variations in water depth also have the potential to alter brGDGT reconstructed MAAT due to variations in integrated water column temperatures (Loomis et al., 2014b), which could greatly affect lakes that have large differences between epi- and hypolimnetic temperatures. Marginal seismic reflectors are also present at Lake Tana during the periods with the lowest Ti (just below 700 cm, 525 and 550 cm, and 400 cm; Marshall et al., 2011), indicating relative lake lowstands during these periods of decreased precipitation. However, given that Lake Tana water column temperatures show ≤ 1 °C variability between the surface and the bottom (Dargahi and Setegn, 2011), it is unlikely that changes in the water depth of Lake Tana had a significant impact on brGDGT distributions.

3.1.2. Influence of changing microbial ecology on brGDGT distributions

In addition to brGDGT variations associated with lithological changes, we note that several samples with low BIT values have much lower reconstructed MAAT values than adjacent samples with a high BIT value. The BIT index was initially proposed as a proxy for terrestrial

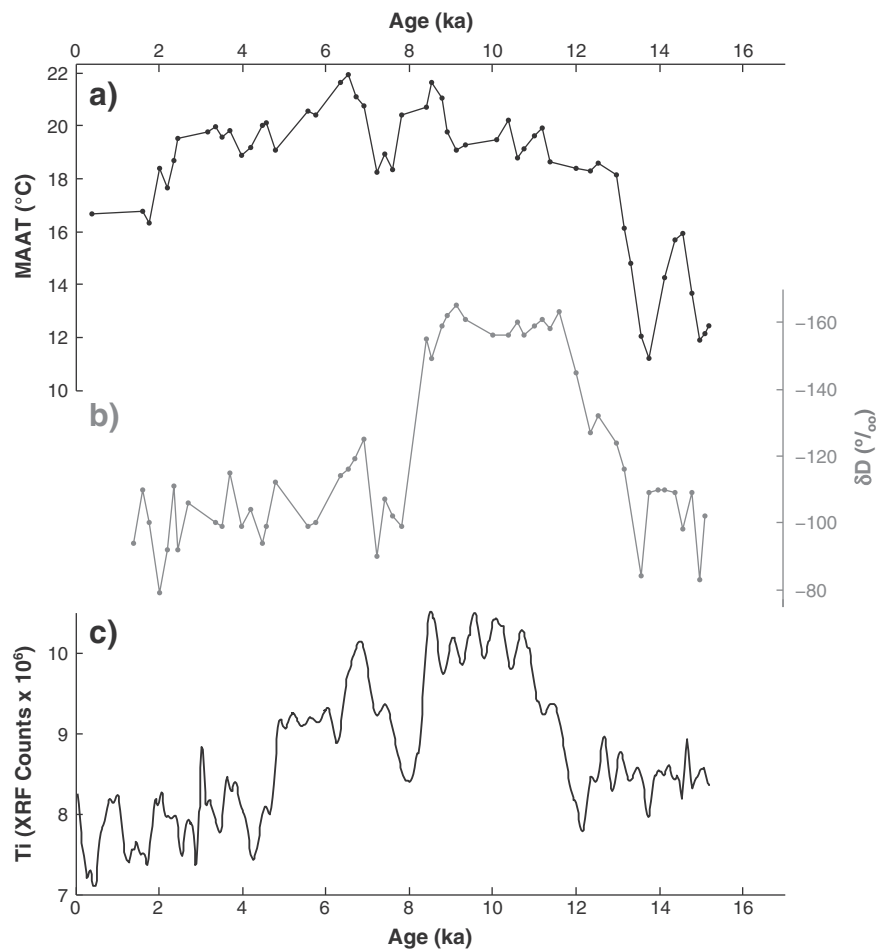


Fig. 4. Temperature and precipitation records from Lake Tana core 03TL3. a) Mean annual air temperature (MAAT; this study), b) δD of leaf waxes (Costa et al., 2014), c) low pass filter of Ti counts (Marshall et al., 2011).

organic matter inputs to marine environments (Hopmans et al., 2004), with higher BIT values (higher relative abundances of brGDGTs) indicating a larger input of soil-derived organic matter relative to aquatically produced organic matter, represented by the relative abundance of crenarchaeol (Sinninghe Damsté et al., 2002). As soil-derived brGDGTs have a different empirical temperature relationship than lacustrine brGDGTs (Tierney et al., 2010; Pearson et al., 2011; Sun et al., 2011; Loomis et al., 2012), large changes in soil-derived organic matter, as defined by the BIT index, have the potential to affect reconstructed temperatures. However, there is strong evidence that brGDGTs in tropical lake sediments are largely derived from production within the lake itself (e.g., Tierney and Russell, 2009; Tierney et al., 2010; Loomis et al., 2011; Buckles et al., 2014b), so BIT values likely record changes in the microbial ecology of lakes, rather than allochthonous vs. autochthonous sources of organic matter in lacustrine environments. Thus, we do not believe that the negative temperature excursions associated with low BIT values are a result of changes in soil-derived organic matter; rather, we suggest that the temperature changes in samples with low BIT are tied to changes in the production of brGDGTs and crenarchaeol in the lake itself.

BrGDGTs are likely produced by heterotrophic acidobacteria (Weijers et al., 2006, 2010; Sinninghe Damsté et al., 2011, 2014), and there is empirical evidence to suggest that brGDGT production increases in deeper, less oxic lake waters (Sinninghe Damsté et al., 2009; Bechtel et al., 2010; Woltering et al., 2012; Buckles et al., 2014b; Loomis et al., 2014b). Crenarchaeol is produced by an ammonia-oxidizing archaea (Francis et al., 2005), and in lakes, peak production of ammonia-oxidizing archaea takes place near the oxycline (Pouliot et al., 2009;

Llirós et al., 2010; Buckles et al., 2013). It seems unlikely that competitive interactions between these two groups could cause changes in the depth of brGDGT production; however, such changes could affect reconstructed temperatures at higher latitudes with large hypolimnetic/epilimnetic temperature gradients. In contrast, water temperature gradients within east African lakes are minimal (<2 °C; Loomis et al., 2014a and references therein), and thus, variations in production depth are not the cause of these large temperature excursions.

While the mechanism linking low BIT to negative temperature anomalies is unknown, we suggest that it likely involves changes in the microbial flora that produce brGDGTs. BIT values in Lake Tana surface sediments are relatively high, indicating relatively low production of crenarchaeol-producing ammonia-oxidizing archaea. Presently, wind speeds at Lake Tana cause nearly constant mixing (Wondie et al., 2007) resulting in only weak seasonal stratification (Wood and Talling, 1988), thereby inhibiting the formation of an oxycline, which would likely suppress the growth of ammonia-oxidizing archaea. It is possible that in the past, changes in wind speed and/or nitrogen cycling in the lake increased production of crenarchaeol, thereby decreasing BIT values. Moreover, there is evidence of human disturbance in the Lake Tana catchment starting near 1.7 ka (177 cm depth; Marshall et al., 2011), which has the capability to alter the nitrogen cycle of the lake (Russell et al., 2009), potentially increasing crenarchaeol production as well. Changes in water column oxygenation and nutrient concentrations alone are likely not the direct cause of the negative temperature excursions, as nutrient and oxygen concentrations do not significantly control brGDGT distributions in East African lakes (Loomis et al., 2014a). However, it is possible that these changes affect the microbial ecology of the lake, including

both the changes in bacterial vs. archaeal populations signified by BIT, as well as the populations of brGDGT-producing bacteria, thereby altering the distributions of brGDGTs deposited in the lake sediments.

At Lake Tana, it appears that brGDGT reconstructed temperatures strongly deviate from the reconstructed temperatures of adjacent samples when BIT are less than 0.5 (Fig. 3). Interestingly, TEX₈₆ reconstructed temperatures in global lakes do not accurately record observed temperatures when BIT > 0.5 (Powers et al., 2010), and reconstructed temperatures from surface sediments in East African rift lakes are on average 10 °C lower than observed temperatures, which also have low BIT values (mean = 0.35; Loomis et al., 2014a). These data could suggest that the shift in microbial ecology when archaeal and bacterial GDGTs are produced at similar rates (theoretical BIT = 0.5) is a critical threshold when applying GDGT-based paleotemperature proxies; however, the exact threshold should be applied cautiously given that a wide range of BIT values can be obtained for the same sample run in different laboratories (Schouten et al., 2013). Furthermore, given the limited number of lakes with low BIT in the global lacustrine TEX₈₆ dataset (Powers et al., 2010) and the fact that the source organism(s) for brGDGTs are yet unknown, it is difficult to ascertain the reason for reconstructed temperature offsets in samples with low BIT, either in modern or in ancient sediments.

Regardless of the mechanism, large changes in BIT do suggest the potential for biases to the brGDGT paleotemperature reconstruction related to changing brGDGT sources. Thus, we will focus our paleoclimatic interpretation of the Lake Tana temperature record only on samples with BIT ≥ 0.5.

3.2. Temperature variability in Northeast Africa from 15 ka to present

Widespread drought in the Afro-Asian monsoon region during Heinrich Stadial 1 (H1; e.g., Stager et al., 2011 and references therein) led to desiccation of Lake Tana (Lamb et al., 2007; Marshall et al., 2011). Flooding at 15.2 ka returned Lake Tana to a lacustrine environment (Fig. 4a), and our brGDGT data indicate reconstructed temperatures of 12.1 °C at this time. Between 15 ka and 13.8 ka, Lake Tana experienced a 3.7 °C oscillation, followed by a rapid temperature increase of ~7 °C in 0.8 ky, resulting in temperatures of 18.1 °C at 13 ka. Temperatures then gradually increased to a maximum of 21.9 °C at 6.6 ka, followed by a gradual cooling to 16.7 °C in the most recent sample at 0.4 ka. This long-term warming and cooling trend during the Holocene was interrupted by a -3 °C temperature oscillation lasting ~1.5 ky and centered at 7.4 ka. Below we discuss this record and its relation to Late Pleistocene and Holocene climate changes on a global and regional scale.

3.2.1. Late Pleistocene

Temperature variability at Lake Tana during the late Pleistocene is broadly consistent with other records of temperature from around North Africa. At the termination of H1, Lake Tana experienced a 3.7 °C warming between 15.2 and 14.5 ka. Sea surface temperature (SST) records from the Red Sea (Arz et al., 2003) and Eastern Mediterranean (Castañeda et al., 2010) show an abrupt ~5 °C warming between 15 ka and 14.5 ka as well (Fig. 5b–c). This warming is consistent with the timing of the Bølling Oscillation recorded in Greenland ice cores (North Greenland Ice Core Project Members, 2004; Fig. 5a), which was driven by the resumption of Atlantic Meridional Overturning Circulation (AMOC) after H1 (McManus et al., 2004), suggesting that abrupt warming observed in much of the northern hemisphere (Shakun et al., 2012) was also felt in northern tropical Africa. In contrast, this abrupt warming is absent from southern and equatorial African continental paleotemperature records (Fig. 6). This could indicate a northern hemispheric temperature history at Lake Tana that is decoupled from that of equatorial and southeastern Africa.

Temperatures in the eastern Mediterranean (Castañeda et al., 2010) and the Red Sea (Arz et al., 2003) remain warm during the subsequent Allerød Oscillation, yet temperatures at Lake Tana decrease to near H1

values at 13.8 ka (Fig. 5). These minimum temperatures are coincident with the Older Dryas cooling event identified between the Bølling and Allerød warm periods. Although identification of the Older Dryas has mainly been limited to North Atlantic and northern Eurasian paleoclimate records, contemporaneous climate events have also been identified in the tropics, including decreased temperatures in the Cariaco basin (Lea et al., 2003) and Lake Albert (Berke et al., 2014), decreased biogenic silica production in Lake Tanganyika (Tierney and Russell, 2007), and increased primary productivity in the Cariaco Basin (Hughen et al., 1996). Hughen et al. (1996) postulate that increased primary productivity in the Cariaco Basin is driven by a strengthening of the trade winds associated with North Atlantic cooling, while Tierney and Russell (2007) attribute the decrease in biogenic silica production to a weakening of the southerly winds that drive upwelling in Tanganyika. The strengthening (weakening) of northerly (southerly) winds may also explain temperature decreases at Lake Tana, as strengthened northerly trade winds transport cool, dry air from the Tibetan Plateau over the Arabian Sea and into northeast Africa.

Following the temperature minimum at 13.8 ka, temperatures at Lake Tana increased to 18.1 °C by 13 ka and remained fairly stable (mean = 18.3 °C, standard deviation = 0.2 °C) into the Holocene (Fig. 6a). The abrupt temperature increase at 13.8 ka is contemporaneous with a 3 °C increase at Sacred Lake (Loomis et al., 2012; Fig. 6b), but is not observed in other paleotemperature records from east Africa (Powers et al., 2005; Tierney et al., 2008; Berke et al., 2012a, 2014; Fig. 6c–e). The abrupt (800 year) nature of this event indicates that changes in local insolation are not likely to be the cause of the temperature increase. Greenhouse gas forcing is also likely not the cause of this warming, as atmospheric CO₂ concentrations varied little between 13.8 and 13.0 ka (Monnin et al., 2001). The temperature increase at 13.8 ka, however, is similar in timing to changes in the temperature and circulation of the Arabian Sea. SSTs off the coast of Oman, recorded by foraminiferal assemblages (Naidu and Malmgren, 2005; Fig. 7d) and TEX₈₆ (Huguet et al., 2006; Fig. 7c), increased rapidly starting near 14 ka. Foraminiferal assemblage data suggests that this increase was mainly driven by increases in winter SSTs (Naidu and Malmgren, 2005). Furthermore, there are large increases in the fractional abundances of dinoflagellates that thrive under high nutrient conditions (Zonneveld et al., 1997; Fig. 7a) along with the foraminifera *Globigerina bulloides* (Naidu and Malmgren, 1996; Fig. 7b), indicating enhanced upwelling at this time. Taken together, these Arabian Sea data indicate an increase in the strength of the Indian Summer Monsoon and a decrease in the intensity of the Indian Winter Monsoon (Naidu and Malmgren, 2005). We hypothesize that the temperature increase at Lake Tana near 14 ka is associated with this shift in Indian Monsoon circulation.

The Indian summer and winter monsoons are driven by differential heating/cooling of the Asian continent compared to the ocean (Hastenrath, 1991). During northern hemisphere summer, the Tibetan Plateau warms rapidly compared to the Indian Ocean, resulting in low pressure over the continent, which drives southwesterly winds (Fig. 1a) and generates the summer monsoon. Conversely, during the winter months, the Tibetan Plateau cools compared to the ocean, reversing the wind direction over the Arabian Sea to northeasterly (Fig. 1b) and generating the winter monsoon. Modern fluctuations in the strength of the monsoons are controlled, in part, by Eurasian snow and ice cover (Hahn and Shukla, 1976; Vernekar et al., 1995). Continental summer temperatures are lower after winters with large snowfall due to the increased albedo and latent heat fluxes associated with snow melt and evaporation. These weaken the summer monsoon, and result in anomalous northeasterly winds and a weakening of the Somali Jet.

Fluctuations in the Somali Jet alter the transport of moist, warm air from the Congo Basin to northeast Africa, affecting precipitation on the Ethiopian Plateau (Camberlin, 1997). Paleoclimate modeling studies focused on this region show that increased ice cover over Eurasia decreases temperatures and precipitation over Northeast Africa due to a strengthening of the northeasterly winds (deMenocal and Rind,

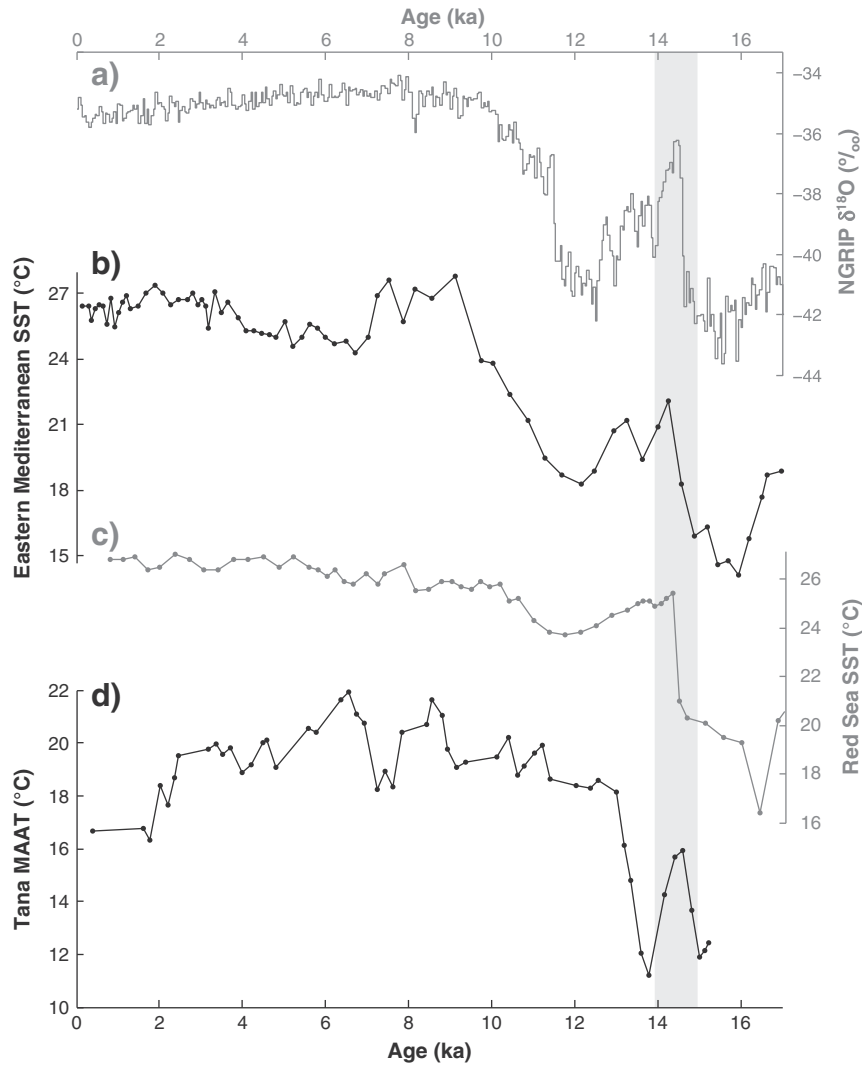


Fig. 5. Comparison of North African temperature records with the Greenland ice core record. a) $\delta^{18}\text{O}$ of the NGRIP ice core (North Greenland Ice Core Project Members, 2004), b) Eastern Mediterranean sea surface temperature (SST; Castañeda et al., 2010), c) Red Sea SST (Arz et al., 2003), and d) Lake Tana mean annual air temperature (MAAT; this study). Gray shading marks the Bølling Oscillation as defined by the NGRIP ice core.

1993; Otto-Bliesner et al., 2014). The onset of a strong Indian summer monsoon at 14 ka would have weakened the easterly trade winds and strengthened the southwesterly winds and the Somali Jet, transporting warm air to the Ethiopian Plateau.

Our hypothesis that large changes in Indian Monsoon circulation trigger changes in temperature at Lake Tana is supported by a leaf wax hydrogen isotope record from Lake Tana (Costa et al., 2014), which shows that the leaf waxes became more D-depleted concomitantly with the rise in temperature (Fig. 4a–b). The temperature increase and the initial onset of the leaf wax δD depletion after 13.8 ka lead increased runoff at Lake Tana (Marshall et al., 2011; Fig. 4c) and in the Nile River catchment (Weldeab et al., 2014) by ~2 ky, but peak leaf wax δD depletion is contemporaneous with peak local and regional runoff. This would suggest that the temperature increase/ δD depletion starting at 13.8 ka was caused by an incursion of warm, δD depleted air masses from the Congo Basin (Costa et al., 2014) to the Ethiopian Plateau, which was subsequently followed by an increase in precipitation over ~2 ky, peaking during the early Holocene, causing additional depletion of the leaf wax isotopes through the amount effect.

Interestingly, although temperatures at Lake Tana appear to be affected by AMOC-induced global climate events early in the deglacial process, including H1 and the Bølling Oscillation, there is no apparent cooling coincident with the Younger Dryas (YD, 12.8–11.5 ka; Fig. 5).

This observation is again consistent with an incursion of Congo Basin air masses onto the Ethiopian Plateau starting at 14 ka, as the Congo Basin temperature record (Weijers et al., 2007b) does not show a temperature decrease associated with the YD.

The linkage between Indian Monsoon circulation and temperature at Lake Tana and Sacred Lake (Loomis et al., 2012) contrasts with temperature records from central equatorial Africa (Tierney et al., 2008; Berke et al., 2012a), where variability is more strongly tied to changes in CO_2 and insolation. Furthermore, the temperature changes associated with Indian Monsoon circulation are more pronounced at Lake Tana (~7 °C) than at Sacred Lake (~3 °C). This would suggest that temperature changes in northeast Africa are more strongly influenced by large changes in atmospheric circulation during the last deglaciation than locations to the south and west.

3.2.2. Holocene

Temperatures at Lake Tana gradually increase from 18.1 °C at 13 ka to 21.9 °C at 6.6 ka, gradually cool to 19.5 °C at 2 ka, and then cool more rapidly to 16.7 °C by the most recent sample at 0.4 ka (Fig. 6a). Broadly, the trends in Holocene temperature at Lake Tana are similar to other equatorial east African paleotemperature records, with the highest reconstructed temperatures during the mid-Holocene and the lowest reconstructed temperatures during the late Holocene (Fig. 5).

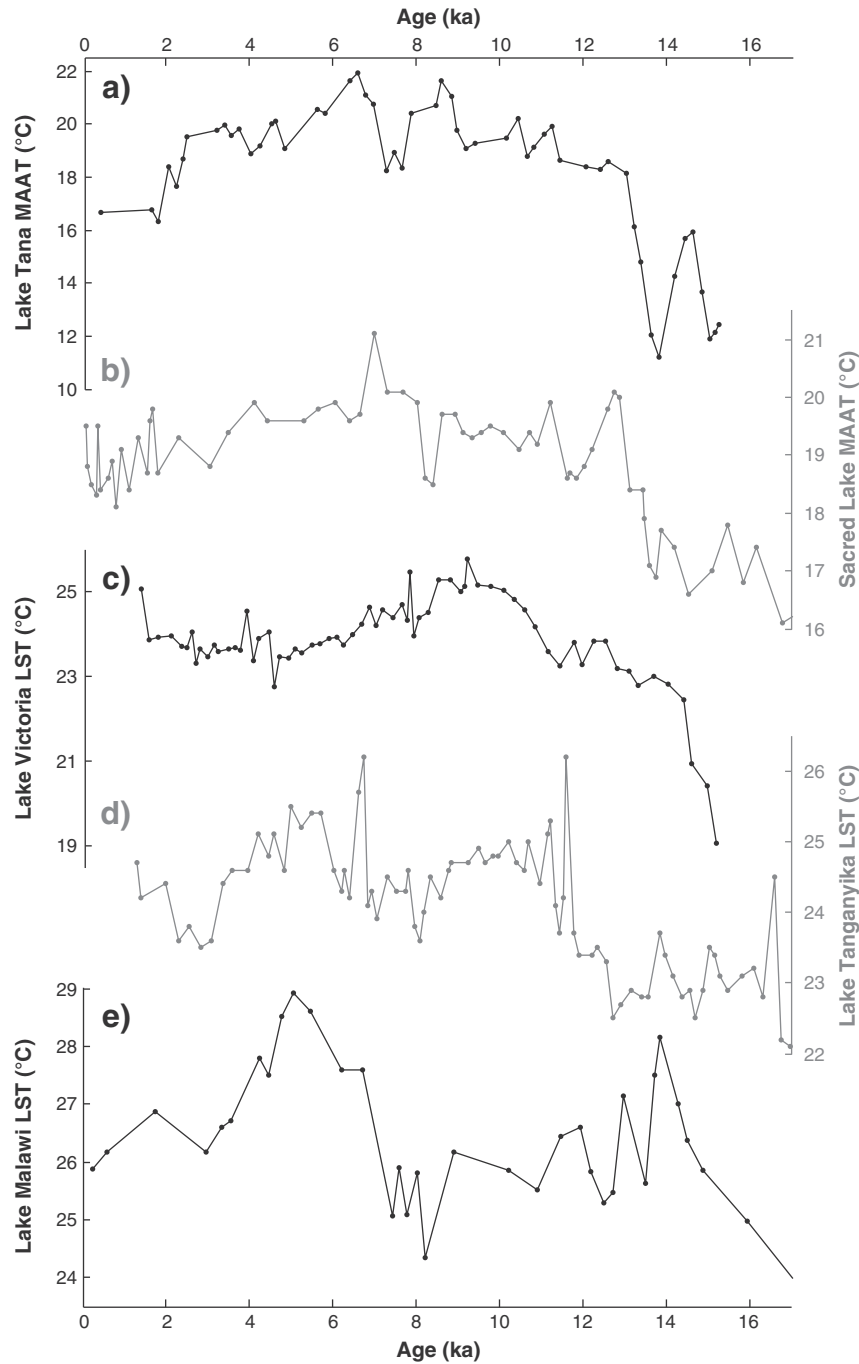


Fig. 6. Comparison of continental East African paleotemperature records. a) Mean annual air temperature (MAAT) at Lake Tana (12.0°N; this study), b) MAAT at Sacred Lake (0°N; Loomis et al., 2012), c) lake surface temperature (LST) at Lake Victoria (1°S; Berke et al., 2012a), d) LST at Lake Tanganyika (7°S; Tierney et al., 2008), and e) LST at Lake Malawi (10°S; Powers et al., 2005).

However, the timing of the mid-Holocene thermal maximum differs among the different records, with maxima near 9 ka at Lake Victoria (Berke et al., 2012a), near 7 ka at Lake Tana and Sacred Lake (Loomis et al., 2012), and near 5 ka at Lakes Malawi (Powers et al., 2005) and Tanganyika (Tierney et al., 2008). Peak mid-Holocene temperatures in Africa are not the result of greenhouse gas radiative forcing, as CO₂ reaches a relative minimum during the mid-Holocene (Indermuhle et al., 1999). The thermal maxima are also not a direct result of local insolation forcing, as peak temperatures at Lake Tana and Sacred Lake lag maximum northern hemisphere summer insolation by ~4 ky, while peak temperatures at Lakes Malawi and Tanganyika lead peak southern hemisphere summer insolation by ~3 ky. Furthermore, east African

temperature variability during the Holocene does not vary systematically with changes in hydrology, as peak temperatures at Lake Tana, Lake Tanganyika, and Lake Victoria occur during a transition from wet to dry conditions (Tierney et al., 2008; Berke et al., 2012a; Costa et al., 2014), while peak temperatures at Lake Malawi (Powers et al., 2005) occur during a transition from dry to wet conditions (Castañeda et al., 2007). Finally, the relative abruptness of mid-Holocene thermal maxima varies between different locations: Lakes Tanganyika and Malawi record temperature increases of 2–3 °C over 2 ky, while temperature maxima at Lake Tana and Sacred Lake are reached through a gradual increase starting at the beginning of the Holocene. Thus, despite the prevalence of warmer mid-Holocene conditions at these sites, the differences in

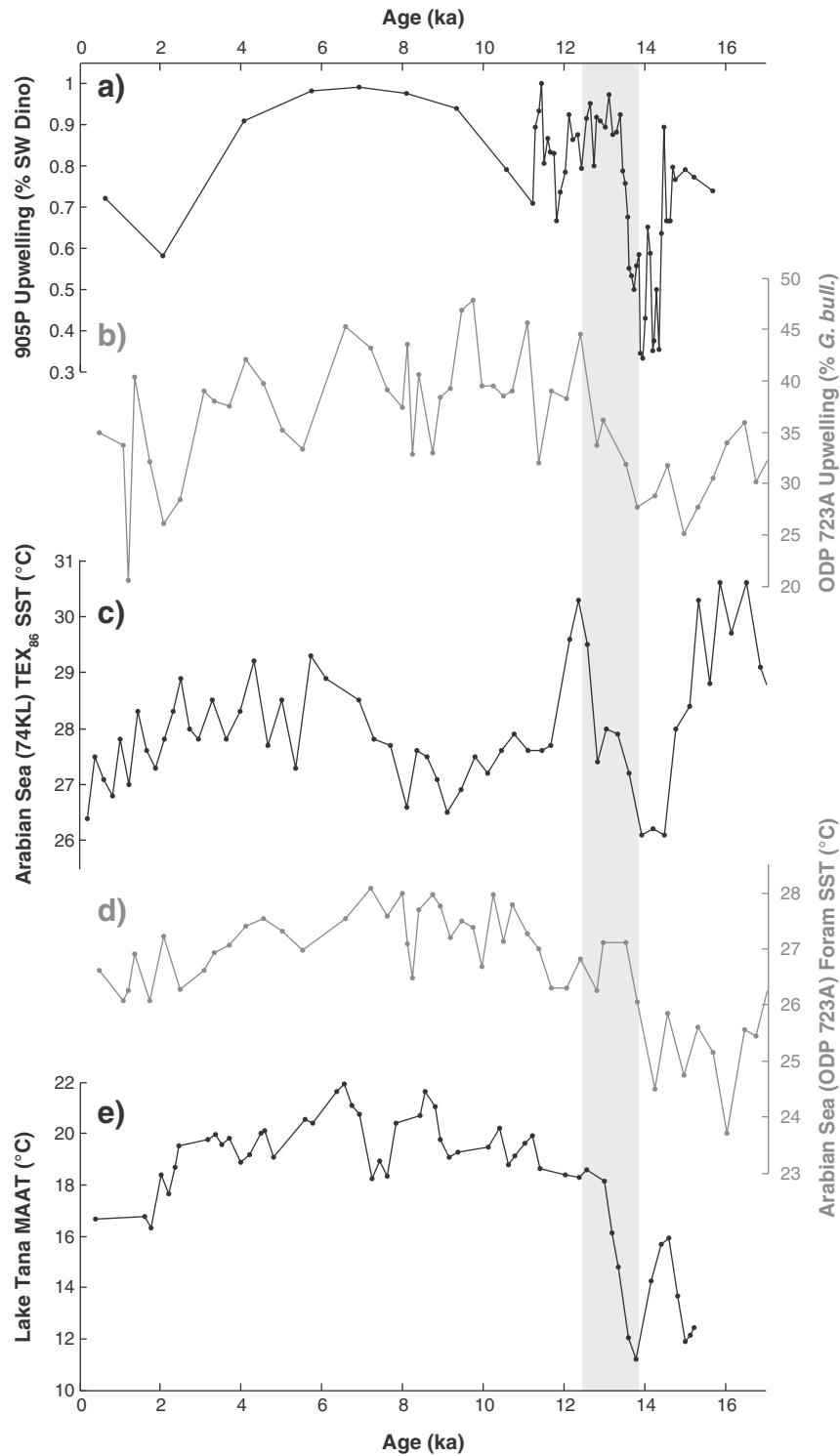


Fig. 7. Comparison of paleoclimate records influenced by the Indian Monsoon. Strength of upwelling in the western Arabian Sea measured by a) the relative abundance of dinoflagellate species with the highest relative abundance during the Indian Summer Monsoon at 905P (Zonneveld et al., 1997) and b) the relative abundance of *G. bulloides* at ODP 723A (Naidu and Malmgren, 1996); sea surface temperature (SST) in the western Arabian Sea reconstructed using c) the TEX_{86} proxy at 74KL (Huguet et al., 2006) and d) foraminifera at ODP 723A (Naidu and Malmgren, 2005); e) mean annual air temperature (MAAT) at Lake Tana (this study). ^{14}C ages from 905P were converted to calendar years using the Marine13 radiocarbon curve (Reimer et al., 2013), and the new age model was constructed using Bacon 2.2 (Blaauw et al., 2007).

timing, relative abruptness, and hydrological linkages indicate that mid-Holocene thermal maxima at different east African locations are likely driven by different mechanisms.

The broad Holocene warming and cooling trend at Lake Tana is interrupted by a 3 °C temperature oscillation over 1.5 ky centered at 7.4 ka. While this oscillation could be associated with the 8.2 ka cooling

event identified in the Greenland ice cores (Alley et al., 1997), the event we observe is outside of age model error of 8.2 ka ($\sigma = 0.37$ ky at this time) and appears to have been much longer-lived than the 8.2 ka event observed in Greenland. This cold oscillation is not apparent in either continental (Fig. 6) or marine (Figs. 5, 7) temperature records from the region, but the onset does align with an abrupt leaf wax δD

enrichment (Costa et al., 2014; Fig. 4b) and a decrease in Ti (Marshall et al., 2011; Fig. 4c), indicating a concomitant drought. In this context, the Ti record from Lake Tana shows that precipitation gradually decreased after 7 ka (Marshall et al., 2011; Fig. 4c), potentially suggesting that the gradual cooling we observe from 7 ka through the late Holocene is linked to regional hydrological change. Although the mechanisms linking temperature and precipitation at Lake Tana are not known, it is possible that reductions in cloud cover and atmospheric humidity stimulated long-wave and latent heat losses, thereby cooling Lake Tana during drier intervals. In any case, our data suggest that the hydrological and thermal histories of northeastern Africa are more intimately linked than hydrological and temperature histories in equatorial and southern Africa. Such a link is plausible, given the strongly monsoonal nature of precipitation in northeastern Africa.

4. Conclusions

We present the first quantitative paleotemperature record from northern Africa using the brGDGT lacustrine paleothermometer to investigate the controls on temperature variability in the northern tropics over the past 15 ka. We find that the thermal history of northeast Africa is distinct from the equatorial and southern tropics, and is instead largely tied to variations in the strength of the monsoons and regional hydrology. The Bølling Oscillation induced a large warming at Lake Tana, which is evident in temperature records from the Red Sea (Arz et al., 2003) and eastern Mediterranean (Castañeda et al., 2010) but is not seen in equatorial and southeast African paleotemperature records. After this oscillation, temperatures warmed near 14 ka, likely due to large-scale reorganization of wind patterns associated with a weakening of the Indian Winter Monsoon and a strengthening of the Indian Summer Monsoon, which greatly diminished the transport of cold, dry air masses from the Tibetan Plateau. Finally, like other east African paleotemperature locations (Powers et al., 2005; Tierney et al., 2008; Berke et al., 2012a; Loomis et al., 2012), Lake Tana experienced a mid-Holocene thermal maximum. However, existing data suggest discrepancies in the timing and magnitude of the mid-Holocene temperature maximum in different regions of Africa, suggesting that this warming arises from diverse causes. Cooling near 7.4 ka, and gradual cooling from the mid-Holocene to present, occur in association with drier conditions, suggesting that, unlike equatorial and southeast Africa, the thermal history of northeast Africa is more directly linked to changes in regional hydrology. Finally, the magnitude of temperature change is larger at Lake Tana compared to other east African locations, potentially due to an amplification of warming at higher latitudes.

Acknowledgments

We would like to thank B. Konecky for helpful discussions and assistance with core sampling, and K. Costa and R. Tarozo for laboratory assistance. This material is based upon work supported by the National Science Foundation under grant number EAR-1226566 to J. Russell and by a Geological Society of America Graduate Student Research Grant awarded to S. Loomis. We also thank two anonymous reviewers for comments that helped to improve earlier drafts of this manuscript.

Appendix A. Supplementary data

Supplementary data to this article can be found online at <http://dx.doi.org/10.1016/j.palaeo.2015.02.005>.

References

Alley, R.B., Mayewski, P.A., Sowers, T., Stuiver, M., Taylor, K.C., Clark, P.U., 1997. Holocene climatic instability: a prominent, widespread event 8200 yr ago. *Geology* 25, 483–486.

Arz, H.W., Patzold, J., Müller, P.J., Moammer, M.O., 2003. Influence of Northern Hemisphere climate and global sea level rise on the restricted Red Sea marine environment during termination I. *Paleoceanography* 18.

Bechtel, A., Smittenberg, R.H., Bernasconi, S.M., Schubert, C.J., 2010. Distribution of branched and isoprenoid tetraether lipids in an oligotrophic and a eutrophic Swiss lake: insights into sources and GDGT-based proxies. *Org. Geochem.* 41, 822–832.

Berke, M.A., Johnson, T.C., Werne, J.P., Grice, K., Schouten, S., Sinninghe Damsté, J.S., 2012a. Molecular records of climate variability and vegetation response since the Late Pleistocene in the Lake Victoria basin, East Africa. *Quat. Sci. Rev.* 55, 59–74.

Berke, M.A., Johnson, T.C., Werne, J.P., Schouten, S., Sinninghe Damsté, J.S., 2012b. A mid-Holocene thermal maximum at the end of the African Humid Period. *Earth Planet. Sci. Lett.* 351, 95–104.

Berke, M.A., Johnson, T.C., Werne, J.P., Livingstone, D.A., Grice, K., Schouten, S., Sinninghe Damsté, J.S., 2014. Characterization of the last deglacial transition in tropical East Africa: insights from Lake Albert. *Palaeogeogr. Palaeoclimatol. Palaeoecol.* 409, 1–8.

Blaauw, M., Bakker, R., Christen, J.A., Hall, V.A., van der Plicht, J., 2007. A Bayesian framework for age modeling of radiocarbon-dated peat deposits: case studies from the Netherlands. *Radiocarbon* 49, 357–367.

Buckles, L.K., Villanueva, L., Weijers, J.W.H., Verschuren, D., Sinninghe Damsté, J.S., 2013. Linking isoprenoidal GDGT membrane lipid distributions with gene abundances of ammonia-oxidizing Thaumarchaeota and uncultured crenarchaeotal groups in the water column of a tropical lake (Lake Challa, East Africa). *Environ. Microbiol.* 15, 2445–2462.

Buckles, L.K., Weijers, J.W.H., Tran, X.M., Waldron, S., Sinninghe Damsté, J.S., 2014a. Provenance of tetraether membrane lipids in a large temperate lake (Loch Lomond, UK): implications for glycerol dialkyl glycerol tetraether (GDGT)-based paleothermometry. *Biogeosciences* 11, 5539–5563.

Buckles, L.K., Weijers, J.W.H., Verschuren, D., Sinninghe Damsté, J.S., 2014b. Sources of core and intact branched tetraether membrane lipids in the lacustrine environment: anatomy of Lake Challa and its catchment, equatorial East Africa. *Geochim. Cosmochim. Acta* 140, 106–126.

Camberlin, P., 1997. Rainfall anomalies in the source region of the Nile and their connection with the Indian summer monsoon. *J. Clim.* 10, 1380–1392.

Castañeda, I.S., Werne, J.P., Johnson, T.C., 2007. Wet and arid phases in the southeast African tropics since the Last Glacial Maximum. *Geology* 35, 823–826.

Castañeda, I.S., Schefuss, E., Patzold, J., Damsté, J.S.S., Weldeab, S., Schouten, S., 2010. Millennial-scale sea surface temperature changes in the eastern Mediterranean (Nile River Delta region) over the last 27,000 years. *Paleoceanography* 25.

Coetzee, J.A., 1967. Pollen analytical studies in East and southern Africa. *Palaeoecol. Afr.* 3, 1–146.

Costa, K., Russell, J., Konecky, B., Lamb, H., 2014. Isotopic reconstruction of the African Humid Period and Congo Air Boundary migration at Lake Tana, Ethiopia. *Quat. Sci. Rev.* 83, 58–67.

Dargahi, B., Setegn, S.G., 2011. Combined 3D hydrodynamic and watershed modelling of Lake Tana, Ethiopia. *J. Hydrol.* 398, 44–64.

deMenocal, P.B., Rind, D., 1993. Sensitivity of Asian and African climate to variations in seasonal insolation, glacial ice cover, sea-surface temperature, and Asian orography. *J. Geophys. Res.-Atmos.* 98, 7265–7287.

Fawcett, P.J., Werne, J.P., Anderson, R.S., Heikoop, J.M., Brown, E.T., Berke, M.A., Smith, S.J., Goff, F., Donohoo-Hurley, L., Cisneros-Dozal, L.M., Schouten, S., Sinninghe Damsté, J.S., Huang, Y.S., Toney, J., Fessenden, J., WoldeGabriel, G., Atudorei, V., Geissman, J.W., Allen, C.D., 2011. Extended megadroughts in the southwestern United States during Pleistocene interglacials. *Nature* 470, 518–521.

Francis, C.A., Roberts, K.J., Beman, J.M., Santoro, A.E., Oakley, B.B., 2005. Ubiquity and diversity of ammonia-oxidizing archaea in water columns and sediments of the ocean. *Proc. Natl. Acad. Sci. U. S. A.* 102, 14683–14688.

Gebrekirstos, A., Worbes, M., Teketay, D., Fetene, M., Mitlohner, R., 2009. Stable carbon isotope ratios in tree rings of co-occurring species from semi-arid tropics in Africa: patterns and climatic signals. *Glob. Planet. Chang.* 66, 253–260.

Hahn, D.G., Shukla, J., 1976. Apparent relationship between Eurasian snow cover and Indian monsoon rainfall. *J. Atmos. Sci.* 33, 2461–2462.

Hastenrath, S., 1991. *Climate Dynamics of the Tropics*. Springer, Dordrecht.

Heegaard, E., Birks, H.J.B., Telford, R.J., 2005. Relationships between calibrated ages and depth in stratigraphical sequences: an estimation procedure by mixed-effect regression. *The Holocene* 15, 612–618.

Hopmans, E.C., Weijers, J.W.H., Schefuß, E., Herfort, L., Sinninghe Damsté, J.S., Schouten, S., 2004. A novel proxy for terrestrial organic matter in sediments based on branched and isoprenoid tetraether lipids. *Earth Planet. Sci. Lett.* 224, 107–116.

Hughen, K.A., Overpeck, J.T., Peterson, L.C., Trumbore, S., 1996. Rapid climate changes in the tropical Atlantic region during the last deglaciation. *Nature* 380, 51–54.

Huguet, C., Kim, J.H., Sinninghe Damsté, J.S., Schouten, S., 2006. Reconstruction of sea surface temperature variations in the Arabian Sea over the last 23 kyr using organic proxies (TEX₈₆ and U₃₇). *Paleoceanography* 21.

Huguet, A., Fosse, C., Laggoun-Defarge, F., Delarue, F., Derenne, S., 2013. Effects of a short-term experimental microclimate warming on the abundance and distribution of branched GDGTs in a French peatland. *Geochim. Cosmochim. Acta* 105, 294–315.

Indermuhle, A., Stocker, T.F., Joos, F., Fischer, H., Smith, H.J., Wahlen, M., Deck, B., Mastroianni, D., Tschumi, J., Blunier, T., Meyer, R., Stauffer, B., 1999. Holocene carbon-cycle dynamics based on CO₂ trapped in ice at Taylor Dome, Antarctica. *Nature* 398, 121–126.

Kebede, S., Travi, Y., Alemayehu, T., Marc, V., 2006. Water balance of Lake Tana and its sensitivity to fluctuations in rainfall, Blue Nile basin, Ethiopia. *J. Hydrol.* 316, 233–247.

Lamb, H.F., Bates, C.R., Coombes, P.V., Marshall, M.H., Umer, M., Davies, S.J., Dejen, E., 2007. Late Pleistocene desiccation of Lake Tana, source of the Blue Nile. *Quat. Sci. Rev.* 26, 287–299.

Lea, D.W., Pak, D.K., Peterson, L.C., Hughen, K.A., 2003. Synchronicity of tropical and high-latitude Atlantic temperatures over the last glacial termination. *Science* 301, 1361–1364.

Llirós, M., Gich, F., Plasencia, A., Auguet, J.C., Darchambeau, F., Casamayor, E.O., Descy, J.P., Borrego, C., 2010. Vertical distribution of ammonia-oxidizing Crenarchaeota and

- methanogens in the epipelagic waters of Lake Kivu (Rwanda–Democratic Republic of the Congo). *Appl. Environ. Microbiol.* 76, 6853–6863.
- Loomis, S.E., Russell, J.M., Sinninghe Damsté, J.S., 2011. Distributions of branched GDGTs in soils and lake sediments from western Uganda: implications for a lacustrine paleothermometer. *Org. Geochem.* 42, 739–751.
- Loomis, S.E., Russell, J.M., Ladd, B., Street-Perrott, F.A., Sinninghe Damsté, J.S., 2012. Calibration and application of the branched GDGT temperature proxy on East African lake sediments. *Earth Planet. Sci. Lett.* 357–358, 277–288.
- Loomis, S.E., Russell, J.M., Eggermont, H., Verschuren, D., Sinninghe Damsté, J.S., 2014a. Effects of temperature, pH and nutrient concentration on branched GDGT distributions in East African lakes: implications for paleoenvironmental reconstruction. *Org. Geochem.* 66, 25–37.
- Loomis, S.E., Russell, J.M., Heuvelink, A.M., D'Andrea, W.J., Damsté, J.S.S., 2014b. Seasonal variability of branched glycerol dialkyl glycerol tetraethers (brGDGTs) in a temperate lake system. *Geochim. Cosmochim. Acta* 144, 173–187.
- Marshall, M.H., Lamb, H.F., Huws, D., Davies, S.J., Bates, R., Bloemendal, J., Boyle, J., Leng, M.J., Umer, M., Bryant, C., 2011. Late Pleistocene and Holocene drought events at Lake Tana, the source of the Blue Nile. *Glob. Planet. Chang.* 78, 147–161.
- McManus, J.F., Francois, R., Gherardi, J.M., Keigwin, L.D., Brown-Leger, S., 2004. Collapse and rapid resumption of Atlantic meridional circulation linked to deglacial climate changes. *Nature* 428, 834–837.
- Monnin, E., Indermuhle, A., Dallenbach, A., Fluckiger, J., Stauffer, B., Stocker, T.F., Raynaud, D., Barnola, J.M., 2001. Atmospheric CO₂ concentrations over the last glacial termination. *Science* 291, 112–114.
- Naidu, P.D., Malmgren, B.A., 1996. A high-resolution record of late quaternary upwelling along the Oman Margin, Arabian Sea based on planktonic foraminifera. *Paleoceanography* 11, 129–140.
- Naidu, P.D., Malmgren, B.A., 2005. Seasonal sea surface temperature contrast between the Holocene and last glacial period in the western Arabian Sea (Ocean Drilling Project Site 723A): modulated by monsoon upwelling. *Paleoceanography* 20.
- Niemann, H., Stadnitskaia, A., Wirth, S.B., Gilli, A., Anselmetti, F.S., Sinninghe Damsté, J.S., Schouten, S., Hopmans, E.C., Lehmann, M.F., 2012. Bacterial GDGTs in Holocene sediments and catchment soils of a high Alpine lake: application of the MBT/CBT-paleothermometer. *Clim. Past* 8, 889–906.
- North Greenland Ice Core Project Members, 2004. High-resolution record of Northern Hemisphere climate extending into the last interglacial period. *Nature* 431, 147–151.
- Otto-Bliesner, B.L., Russell, J.M., Clark, P.U., Liu, Z.Y., Overpeck, J.T., Konecky, B., deMenocal, P., Nicholson, S.E., He, F., Lu, Z.Y., 2014. Coherent changes of southeastern equatorial and northern African rainfall during the last deglaciation. *Science* 346, 1223–1227.
- Pearson, E.J., Juggins, S., Talbot, H.M., Weckstrom, J., Rosen, P., Ryves, D.B., Roberts, S.J., Schmidt, R., 2011. A lacustrine GDGT-temperature calibration from the Scandinavian Arctic to Antarctica: renewed potential for the application of GDGT-paleothermometry in lakes. *Geochim. Cosmochim. Acta* 75, 6225–6238.
- Peterse, F., Hopmans, E.C., Schouten, S., Mets, A., Rijpstra, W.I.C., Sinninghe Damsté, J.S., 2011. Identification and distribution of intact polar branched tetraether lipids in peat and soil. *Org. Geochem.* 42, 1007–1015.
- Pouliot, J., Galand, P.E., Lovejoy, C., Vincent, W.F., 2009. Vertical structure of archaeal communities and the distribution of ammonia monooxygenase A gene variants in two meromictic High Arctic lakes. *Environ. Microbiol.* 11, 687–699.
- Powers, L.A., Johnson, T.C., Werne, J.P., Castañeda, I.S., Hopmans, E.C., Sinninghe Damsté, J.S., Schouten, S., 2005. Large temperature variability in the southern African tropics since the Last Glacial Maximum. *Geophys. Res. Lett.* 32, L08706.
- Powers, L.A., Werne, J.P., Vanderwoude, A.J., Sinninghe Damsté, J.S., Hopmans, E.C., Schouten, S., 2010. Applicability and calibration of the TEX₈₆ paleothermometer in lakes. *Org. Geochem.* 41, 404–413.
- Reimer, P.J., Bard, E., Bayliss, A., Beck, J.W., Blackwell, P.G., Ramsey, C.B., Buck, C.E., Cheng, H., Edwards, R.L., Friedrich, M., Grootes, P.M., Guilderson, T.P., Hafflidason, H., Hajdas, I., Hatte, C., Heaton, T.J., Hoffmann, D.L., Hogg, A.G., Hughen, K.A., Kaiser, K.F., Kromer, B., Manning, S.W., Niu, M., Reimer, R.W., Richards, D.A., Scott, E.M., Southon, J.R., Staff, R.A., Turney, C.S.M., van der Plicht, J., 2013. Intcal13 and Marine13 radiocarbon age calibration curves 0–50,000 years cal BP. *Radiocarbon* 55, 1869–1887.
- Russell, J.M., McCoy, S.J., Verschuren, D., Bessems, I., Huang, Y., 2009. Human impacts, climate change, and aquatic ecosystem response during the past 2000 yr at Lake Wandakara, Uganda. *Quat. Res.* 72, 315–324.
- Schmittner, A., Urban, N.M., Shakun, J.D., Mahowald, N.M., Clark, P.U., Bartlein, P.J., Mix, A.C., Rosell-Mele, A., 2011. Climate sensitivity estimated from temperature reconstructions of the Last Glacial Maximum. *Science* 334, 1385–1388.
- Schouten, S., Hopmans, E.C., Schefuß, E., Sinninghe Damsté, J.S., 2002. Distributional variations in marine crenarchaeotal membrane lipids: a new tool for reconstructing ancient sea water temperatures? *Earth Planet. Sci. Lett.* 204, 265–274.
- Schouten, S., Hopmans, E.C., Rosell-Mele, A., Pearson, A., Adam, P., Bauersachs, T., Bard, E., Bernasconi, S.M., Bianchi, T.S., Brocks, J.J., Carlson, L.T., Castañeda, I.S., Derenne, S., Selver, A.D., Dutta, K., Eglinton, T., Fosse, C., Galy, V., Grice, K., Hinrichs, K.U., Huang, Y.S., Huguet, A., Huguet, C., Hurley, S., Ingalls, A., Jia, G., Keely, B., Knappy, C., Kondo, M., Krishnan, S., Lincoln, S., Lipp, J., Mangelsdorf, K., Martinez-Garcia, A., Menot, G., Mets, A., Mollenhauer, G., Ohkouchi, N., Ossebaar, J., Paganini, M., Pancost, R.D., Pearson, E.J., Peterse, F., Reichart, G.J., Schaeffer, P., Schmitt, G., Schwark, L., Shah, S.R., Smith, R.W., Smittenberger, R.H., Summons, R.E., Takano, Y., Talbot, H.M., Taylor, K.W.R., Tarozo, R., Uchida, M., van Dongen, B.E., Van Mooy, B.A.S., Wang, J.X., Warren, C., Weijers, J.W.H., Werne, J.P., Woltering, M., Xie, S.C., Yamamoto, M., Yang, H., Zhang, C.L., Zhang, Y.G., Zhao, M.X., Sinninghe Damsté, J.S., 2013. An interlaboratory study of TEX₈₆ and BIT analysis of sediments, extracts, and standard mixtures. *Geochim. Geophys. Geosyst.* 14, 5263–5285.
- Shakun, J.D., Clark, P.U., He, F., Marcott, S.A., Mix, A.C., Liu, Z.Y., Otto-Bliesner, B., Schmittner, A., Bard, E., 2012. Global warming preceded by increasing carbon dioxide concentrations during the last deglaciation. *Nature* 484, 49–54.
- Sinninghe Damsté, J.S., Hopmans, E.C., Pancost, R.D., Schouten, S., Geenevasen, J.A.J., 2000. Newly discovered non-isoprenoid glycerol dialkyl glycerol tetraether lipids in sediments. *Chem. Commun.* 1683–1684.
- Sinninghe Damsté, J.S., Schouten, S., Hopmans, E.C., van Duin, A.C.T., Geenevasen, J.A.J., 2002. Crenarchaeol: the characteristic core glycerol dibiphytanyl glycerol tetraether membrane lipid of cosmopolitan pelagic crenarchaeota. *J. Lipid Res.* 43, 1641–1651.
- Sinninghe Damsté, J.S., Ossebaar, J., Abbas, B., Schouten, S., Verschuren, D., 2009. Fluxes and distribution of tetraether lipids in an equatorial African lake: constraints on the application of the TEX₈₆ paleothermometer and BIT index in lacustrine settings. *Geochim. Cosmochim. Acta* 73, 4232–4249.
- Sinninghe Damsté, J.S., Rijpstra, W.I.C., Hopmans, E.C., Weijers, J.W.H., Foessel, B.U., Overman, J., Dedysh, S.N., 2011. 13,16-Dimethyl octacosanedionic acid (iso-diabolic acid): a common membrane-spanning lipid of Acidobacteria subdivisions 1 and 3. *Appl. Environ. Microbiol.* 77, 4147–4154.
- Sinninghe Damsté, J.S., Rijpstra, W.I.C., Hopmans, E.C., Foessel, B.U., Wüst, P.K., Overman, J., Tank, M., Bryant, D.A., Dunfield, P.F., Houghton, K., Stott, M.B., 2014. Ether- and ester-bound iso-diabolic acid and other lipids in members of Acidobacteria subdivision 4. *Appl. Environ. Microbiol.* 80, 5207–5218.
- Stager, J.C., Ryves, D.B., Chase, B.M., Pausata, F.S.R., 2011. Catastrophic drought in the Afro-Asian monsoon region during Heinrich Event 1. *Science* 331, 1299–1302.
- Sun, Q., Chu, G., Liu, M., Xie, M., Li, S., Ling, Y., Wang, X., Shi, L., Jia, G., Lü, H., 2011. Distributions and temperature dependence of branched glycerol dialkyl glycerol tetraethers in recent lacustrine sediments from China and Nepal. *J. Geophys. Res.* 116, G01008.
- Thompson, L.G., Mosley-Thompson, E., Davis, M.E., Henderson, K.A., Brecher, H.H., Zagorodnov, V.S., Mashitota, T.A., Lin, P.N., Mikhalenko, V.N., Hardy, D.R., Beer, J., 2002. Kilimanjaro ice core records: evidence of Holocene climate change in tropical Africa. *Science* 298, 589–593.
- Tierney, J.E., Russell, J.M., 2007. Abrupt climate change in southeast tropical Africa influenced by Indian monsoon variability and ITCZ migration. *Geophys. Res. Lett.* 34.
- Tierney, J.E., Russell, J.M., 2009. Distributions of branched GDGTs in a tropical lake system: implications for lacustrine application of the MBT/CBT paleoproxy. *Org. Geochem.* 40, 1032–1036.
- Tierney, J.E., Russell, J.M., Huang, Y., Sinninghe Damsté, J.S., Hopmans, E.C., Cohen, A.S., 2008. Northern hemisphere controls on tropical southeast African climate during the past 60,000 years. *Science* 322, 252–255.
- Tierney, J.E., Russell, J.M., Eggermont, H., Hopmans, E.C., Verschuren, D., Sinninghe Damsté, J.S., 2010. Environmental controls on branched tetraether lipid distributions in tropical East African lake sediments. *Geochim. Cosmochim. Acta* 74, 4902–4918.
- Tierney, J.E., Schouten, S., Pitcher, A., Hopmans, E.C., Sinninghe Damsté, J.S., 2012. Core and intact polar glycerol dialkyl glycerol tetraethers (GDGTs) in Sand Pond, Warwick, Rhode Island (USA): insights into the origin of lacustrine GDGTs. *Geochim. Cosmochim. Acta* 77, 561–581.
- Vernekar, A.D., Zhou, J., Shukla, J., 1995. The effect of Eurasian snow cover on the Indian monsoon. *J. Clim.* 8, 248–266.
- Wang, H.Y., Liu, W.G., Zhang, C.L.L., Wang, Z., Wang, J.X., Liu, Z.H., Dong, H.L., 2012. Distribution of glycerol dialkyl glycerol tetraethers in surface sediments of Lake Qinghai and surrounding soil. *Org. Geochem.* 47, 78–87.
- Weijers, J.W.H., Schouten, S., Hopmans, E.C., Geenevasen, J.A.J., David, O.R.P., Coleman, J.M., Pancost, R.D., Sinninghe Damsté, J.S., 2006. Membrane lipids of mesophilic anaerobic bacteria thriving in peats have typical archaeal traits. *Environ. Microbiol.* 8, 648–657.
- Weijers, J.W.H., Schouten, S., van den Donker, J.C., Hopmans, E.C., Sinninghe Damsté, J.S., 2007a. Environmental controls on bacterial tetraether membrane lipid distribution in soils. *Geochim. Cosmochim. Acta* 71, 703–713.
- Weijers, J.W.H., Schefuß, E., Schouten, S., Sinninghe Damsté, J.S., 2007b. Coupled thermal and hydrological evolution of tropical Africa over the last deglaciation. *Science* 315, 1701–1704.
- Weijers, J.W.H., Panoto, E., van Bleijswijk, J., Schouten, S., Rijpstra, W.I.C., Balk, M., Stams, A.J.M., Sinninghe Damsté, J.S., 2009. Constraints on the biological source(s) of the orphan branched tetraether membrane lipids. *Geomicrobiol. J.* 26, 402–414.
- Weijers, J.W.H., Wiesenberg, G.L.B., Bol, R., Hopmans, E.C., Pancost, R.D., 2010. Carbon isotopic composition of branched tetraether membrane lipids in soils suggest a rapid turnover and a heterotrophic life style of their source organism(s). *Biogeochem. Discuss.* 7, 3691–3734.
- Weldeab, S., Menke, V., Schmiedl, G., 2014. The pace of East African monsoon evolution during the Holocene. *Geophys. Res. Lett.* 41, 1724–1731.
- Woltering, M., Johnson, T.C., Werne, J.P., Schouten, S., Sinninghe Damsté, J.S., 2011. Late Pleistocene temperature history of Southeast Africa: a TEX₈₆ temperature record from Lake Malawi. *Palaeogeogr. Palaeoclimatol. Palaeoecol.* 303, 93–102.
- Woltering, M., Werne, J.P., Kish, J.L., Hicks, R., Sinninghe Damsté, J.S., Schouten, S., 2012. Vertical and temporal variability in concentration and distribution of thaumarchaeotal tetraether lipids in Lake Superior and the implications for the application of the TEX₈₆ temperature proxy. *Geochim. Cosmochim. Acta* 87, 136–153.
- Woltering, M., Atahan, P., Grice, K., Heijnis, H., Taffs, K., Dodson, J., 2014. Glacial and Holocene terrestrial temperature variability in subtropical east Australia as inferred from branched GDGT distributions in a sediment core from Lake McKenzie. *Quat. Res.* 82, 132–145.
- Wondie, A., Mengistu, S., Vijverberg, J., Dejen, E., 2007. Seasonal variation in primary production of a large high altitude tropical lake (Lake Tana, Ethiopia): effects of nutrient availability and water transparency. *Aquat. Ecol.* 41, 195–207.
- Wood, R.B., Talling, J.F., 1988. Chemical and algal relationships in a salinity series of Ethiopian inland waters. *Hydrobiologia* 158, 29–67.
- Zonneveld, K.A.F., Ganssen, G., Troelstra, S., Versteegh, G.J.M., Visscher, H., 1997. Mechanisms forcing abrupt fluctuations of the Indian Ocean summer monsoon during the last deglaciation. *Quat. Sci. Rev.* 16, 187–201.